Binder, B. J. and Cox, Stephen M. A mixer design for the pigtail braid. Fluid Dynamics Research . ISSN 0169-5983 (In Press)

A mixer design for the pigtail braid

B. J. Binder

School of Mathematical Sciences, University of Adelaide, Adelaide 5005, Australia

S. M. Cox *

School of Mathematical Sciences, University of Nottingham,
Nottingham NG7 2RD, UK

Abstract

The stirring of a body of viscous fluid using multiple stirring rods is known to be particularly effective when the rods trace out a path corresponding to a nontrivial mathematical braid. The *optimal* braid is the so-called "pigtail braid", in which three stirring rods execute the usual "over–under" motion associated with braiding (plaiting) hair. We show how to achieve this optimal braiding motion straightforwardly: one stirring rod is driven in a figure-of-eight motion, while the other two rods are baffles, which rotate episodically about their common centre. We also explore the extent to which the physical baffles may be replaced by flow structures (such as periodic islands).

Key words: chaotic advection, braid, Stokes flow, fluid mixing

1 Introduction

This paper concerns laminar mixing of a viscous fluid in a batch mixer. A simple conceptual model for a batch mixer comprises a vat of fluid which is stirred by means of a number of stirring rods. The central design problem, addressed here, is then to devise an effective *stirring protocol* for the mixer, i.e.,

---

* Corresponding author: tel. +44 115 951 4930; fax +44 115 951 3837
   Email addresses: `ben.binder@adelaide.edu.au` (B. J. Binder),
`stephen.cox@nottingham.ac.uk` (S. M. Cox).
   URLs: `http://www.maths.adelaide.edu.au/applied/staff/bbinder.html`
(B. J. Binder), `http://www.maths.nottingham.ac.uk/personal/smc/` (S. M. Cox).

a manner in which the stirring rods should move to maximize some measure of the mixing quality.

It is well known [1,2] that even laminar fluid flows can stir a fluid effectively, provided that the Lagrangian particle paths are chaotic. However, it is an unfortunate fact of life that the stirring quality of the resulting flow can be drastically altered by changes to the parameters such as the relative diameters of the vat and rods, the precise path followed by the stirring rods while executing their protocol, or the cross-sectional profiles of the vat or rods.

Some renewed hope of designing *robust* mixing devices, which are not so sensitive to the vagaries of "accidental" parameter variations was provided recently by Boyland, Aref and Stremler [4], who pointed out, on the basis of Thurston–Nielsen theory, that a certain rate of material line stretch can be guaranteed if at least three stirring rods are used, and if they execute a motion corresponding to a nontrivial mathematical braid. The resulting flows appear in practice to possess a significant region in which the lower bound on the line stretch rate is achieved or exceeded [11], given only the topology of the boundary motions that generate the flow (although the underlying Thurston–Nielsen theory does not predict the size of this region, merely its existence). A recent review is provided by Thiffeault and Finn [16].

For three stirring elements, the optimal braid word, in the sense that it maximizes an appropriately defined entropy, is the "pigtail braid" [7]. (We stress here that the concept of optimality is used throughout this paper only in a certain restricted sense, which is explained more explicitly below, at the end of Section 2.) However, it seems difficult to design a mixer that achieves such a braid and is also simple to construct. We demonstrate in this paper one straightforward means for accomplishing the pigtail braid using simple technology: a single stirring rod together with a pair of baffles that can rotate on a turntable.

The structure of the paper is as follows. In Section 2 we briefly introduce some concepts and notation associated with mathematical braids, and summarize some results pertinent for our fluid mechanical application. In Section 3 we demonstrate our design for implementation of the pigtail braid. Numerical simulations of Stokes flow in our device are described in Section 4, where we compare our results with theoretical predictions. We shall see that flow structures such as periodic orbits (and associated regular islands in the flow) act as barriers to transport and thus effectively serve as additional baffles; such flow structures have recently been named "ghost rods" [12]. Our conclusions are drawn in Section 5.

2 Mathematical background

We consider batch mixing devices that comprise a vat of fluid stirred by m stirring elements. These stirring elements are either mobile stirring rods or baffles. (It turns out, somewhat counterintuitively, that the judicious introduction of baffles, usually stationary, can significantly improve the mixing.) Our model will assume two-dimensional flow, and to simplify matters still further, the vat and the stirring rods will all have circular cross-section.

As the stirring rods move, the topology of their motion relative to each other and to the baffles is usefully described using the mathematical language of braids. We therefore begin by briefly recalling some necessary terminology relating to braids. A more comprehensive account, again from the perspective of applications in fluid mechanics, is given in [4].

We suppose that initially the stirring elements are arranged in some order, from left to right according to some observer. Then the motion of the stirring rods may be characterized topologically in terms of successive interchanges in their order. For instance, the interchange of the jth and $(j + 1)$th stirring elements (counting from the left), clockwise, is represented by the symbol σ_j, called a "braid letter"; a corresponding anticlockwise interchange is denoted by σ_j^{-1}.

All of our stirring protocols are time-periodic, and the sequence of braid letters corresponding to the full sequence of stirrer interchanges during one period is the "braid word". In this paper, braid words are to be read from right to left, although the opposite convention is followed in some other accounts. For example, the braid word $\sigma_1 \sigma_2^{-1}$, for $m = 3$, means that first the middle and rightmost stirring elements are interchanged in an anticlockwise fashion, then the (new) middle and leftmost stirring elements are interchanged clockwise. Braid words may often be simplified, using the following rules: (i) $\sigma_j^{-1} \sigma_j = \sigma_j \sigma_j^{-1} = 1$, where 1 is the identity braid; (ii) $\sigma_{j-1} \sigma_j \sigma_{j-1} = \sigma_j \sigma_{j-1} \sigma_j$; (iii) for $|i - j| \geq 2$, $\sigma_i \sigma_j = \sigma_j \sigma_i$. In what follows, we shall have at most three stirring elements, so that $m \leq 3$, and the last rule will not apply.

It seems inappropriate in a paper of this length to attempt a full description of Thurston–Nielsen theory; a description in a fluid mechanical context, and further references to the literature may be found in [4], whose pertinent results we now summarize. For our purposes it is sufficient to note that the only input to the theory is the topology of the motions of the stirring elements and the fact that the fluid to be mixed is a continuum. No details of the constitutive relation (or, specifically, of the Reynolds number for a Newtonian fluid) are required. An output of the theory is a classification of the stirring protocol into one of three classes, of which the one of most current interest is the pseudo-Anosov, or "p-A", class. Any protocol in the p-A class has associated with it a dilatation

parameter λ, which is a stretching factor enjoyed by (certain) material lines during each period. The value of λ is independent of the material properties of the fluid being mixed, and of any details of the stirring protocol except its braid word, and thus the theory is rather powerful. Of course, from topological considerations alone it is not possible to predict the *size* of the region of the flow domain enjoying the predicted dilatation. From a practical perspective, this is a severe limitation, and one which necessitates corresponding numerical simulations (or experiments), whose results for the size of the mixing region are then specific to the model (or flow regime) concerned. In this paper, for definiteness, we describe numerical simulations of Stokes flow (creeping flow). The Stokes flow regime possesses some significant advantages for numerical simulations (for example, uniqueness of the flow, given the boundary motions, and the relative simplicity of simulation in a time-varying geometry).

For $m = 3$, each braid letter has a corresponding matrix, which can be used in determining the line stretch rate associated with any given braid word. We have, corresponding to σ_1 and σ_2, respectively,

$$s_1 = \begin{pmatrix} 1 & -1 \\ 0 & 1 \end{pmatrix}, \quad s_2 = \begin{pmatrix} 1 & 0 \\ 1 & 1 \end{pmatrix}.$$

The corresponding matrix for σ_j^{-1} is simply s_j^{-1} (for $j = 1, 2$). The matrix associated with a braid word is then the product of the matrices associated with the component braid letters. For example the braid word $\sigma_1\sigma_1\sigma_2^{-1}\sigma_2^{-1}$ is associated with the matrix

$$s_1 s_1 s_2^{-1} s_2^{-1} = \begin{pmatrix} 5 & -2 \\ -2 & 1 \end{pmatrix}. \tag{1}$$

The dilatation λ is predicted by the spectral radius (i.e., the larger of the magnitudes of the two eigenvalues) of the associated braid matrix. For $s_1 s_1 s_2^{-1} s_2^{-1}$, $\lambda = 3 + \sqrt{8} \approx 5.8$. If the spectral radius of the braid matrix is unity, the corresponding braid is said to be trivial (i.e., not in the p-A class).

It has been shown [7] that for three stirring elements in a bounded domain, such as here, the optimal braid is the so-called pigtail braid $\sigma_1\sigma_2^{-1}$ [4], which has $\lambda = \lambda_{\max} \equiv (3 + \sqrt{5})/2 \approx 2.62$. Here "max" refers to the maximum dilatation over braid words comprising two braid letters; such a notation reflects the definition of optimality used in this paper, namely "providing the maximal dilatation per braid letter". (The restriction to a bounded domain is significant – for example, Thiffeault and Finn [16] show how $\lambda_{\max}$ may be exceeded in a *spatially periodic* mixing device.) Furthermore, in a bounded domain the largest λ for a braid word of length n constructed from σ_1 and σ_2^{-1}

4

is obtained by taking these two braid letters alternately. However, the pigtail braid is difficult to generate with a mechanically simple device. We show in the next section how to devise a stirring protocol with braid word of the form $(\sigma_1\sigma_2^{-1})^n$ for some positive integer n, which should also be straightforward to construct.

3 A simple batch mixer design for the pigtail braid

In this section we give details of a simple batch mixer design that generates the pigtail braid.

Before we proceed further, we make a brief comment on a naming convention used below. We generally follow convention and use the term "stirring rod" for a rod that moves through the fluid, and "baffle" for a similar rod, but stationary. Thus there is a clear distinction between two otherwise identical objects: one moves, and the other does not. However, an exception to this nomenclature arises in the mixer design given below that executes the pigtail braid, in which it is necessary at some phase of the stirring protocol for the baffles themselves to move! One might then reasonably query the usefulness of maintaining both terms, since the words "stirring rod" and "baffle" become effectively interchangeable. However, we believe that it is useful to maintain the distinction that the former means "rod whose primary role is to be driven through the fluid to stir it" while the latter means "rod generally kept fixed, except in rare circumstances, where it must move in order to enable us to achieve the pigtail braid". Although we have found it useful ourselves, we acknowledge that the distinction is slight, once one allows baffles to move occasionally during a stirring protocol.

We begin by considering a simple figure-of-eight motion for a single stirring rod. Clearly such a motion is in itself topologically trivial, but it can generate a nontrivial mathematical braid if a baffle is introduced into each loop [5]. If the baffles remain stationary then in each period we generate the braid word $\sigma_1\sigma_1\sigma_2^{-1}\sigma_2^{-1}$, whose associated matrix is given in (1), and which therefore has dilatation $\lambda \approx 5.8$ [5]. However, this design can readily be modified to generate three pigtail braids per period, and hence $\lambda = \lambda_{\max}^3 \approx 17.94$, as follows. The initial configuration of stirring elements is shown in figure 1(a): the solid circles represent the baffles, and the open circle the stirring rod. The pigtail-braid protocol starts with the stirring rod executing one-half of a figure-of-eight motion, as illustrated in figure 1(b). Next, the two baffles are rotated through 180° about the centre of the vat, anticlockwise — see figure 1(c). This interchange is crucial in obtaining the pigtail braid. The remainder of the protocol involves first the stirring rod completing its figure-of-eight — see figure 1(d) — then a final, clockwise rotation of the baffles through 180° about
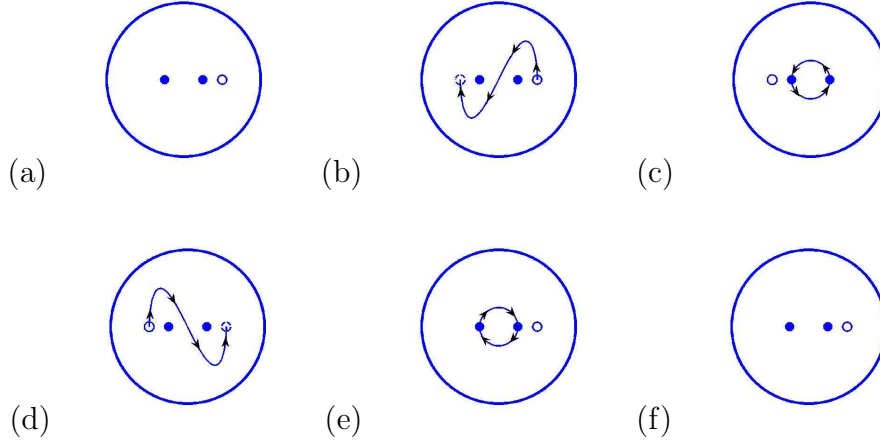
Fig. 1. Stirring protocol and baffle placement to achieve the pigtail braid $(\sigma_1\sigma_2^{-1})^3$. Solid circles represent baffles; the open circle represents the stirring rod. (a) Initial positions of rod and baffles. The stirring protocol comprises (b) half a figure-of-eight motion of the stirring rod, (c) a counterclockwise rotation through 180° of the baffles, (d) the remainder of the figure-of-eight motion of the rod, and finally (e) a clockwise rotation of the baffles, to return all stirring elements to (f) their original positions.

the centre of the vat — see figure 1(e). Thus all stirring elements return to their original locations (figure 1(f)). It is readily determined that the braid word for this protocol is $(\sigma_1\sigma_2^{-1})^3$.

In order to demonstrate the stirring effectiveness of the mixer design described above, we simulate the corresponding slow viscous flow (Stokes flow). We assume that the mixing vat is filled with an incompressible Newtonian viscous fluid, and that the flow is two-dimensional. Our notation closely follows that of [10,11]. It is convenient to work in complex variables, with $z = x + iy$, where x and y are Cartesian coordinates. The origin is chosen as the centre of the vat (which is assumed to be fixed), and lengths have been scaled so that the vat has unit radius, with boundary $|z| = 1$. The stirring elements have circular cross-section, with centres at $p_j(t)$ and radii a_j, for $j = 1 \ldots m$. For simplicity, the angular velocities of the stirrers about their respective axes are set to zero in all simulations. For Stokes flow, at vanishing Reynolds number, the streamfunction ψ satisfies the biharmonic equation $\nabla^4\psi = 0$ [14], whose means of solution in this multiply connected domain is described elsewhere [11]. We now describe the various stirring protocols used in the remainder of the paper.

3.1 Stirring protocols

Here we give details of the stirring protocols considered here. In each case, with no loss of generality, we normalize the period of the protocol to be unity.

Protocol 1 is a figure-of-eight stirring protocol with a single stirring element;

6

thus $m = 1$. The stirring rod has its centre at

$$p_1(t) = A \cos 2\pi t + iA \sin 4\pi t \tag{2}$$

for $0 \leq t \leq 1$; the value of A will be specified below. This protocol is topologically trivial, because $m = 1$.

Protocol 2 is a figure-of-eight stirring protocol with two stationary baffles. Now $m = 3$: the index 1 refers to the stirring rod, while 2 and 3 refer to the stationary baffles. For $0 \leq t \leq 1$, the stirring rod again executes the path given in (2), while the baffles are centred at $p_2(t) = R$ and $p_3(t) = -R$, where R will be specified below. Note that $0 < R < A$ so that one baffle lies in each of the loops of the figure-of-eight.

Protocol 3 is the figure-of-eight stirring protocol described above, and illustrated in figure 1, that generates the pigtail braid. Here the figure-of-eight motion of the stirring rod is punctuated by the episodic rotations of the two "baffles". It is convenient to describe the protocol as follows. For $0 \leq t < 1/4$,

$$p_1(t) = A \cos 4\pi t + iA \sin 8\pi t, \qquad p_2(t) = R;$$

for $1/4 \leq t < 1/2$,

$$p_1(t) = -A, \qquad p_2(t) = -R \cos 4\pi t - iR \sin 4\pi t;$$

for $1/2 \leq t < 3/4$,

$$p_1(t) = -A \cos 4\pi t + iA \sin 8\pi t, \qquad p_2(t) = -R;$$

for $3/4 \leq t \leq 1$,

$$p_1(t) = A, \qquad p_2(t) = R \cos 4\pi t - iR \sin 4\pi t.$$

At all stages, $p_3(t) = -p_2(t)$.

In addition, we shall compare results with two further protocols: Protocols 2* and 3*. These are identical, respectively, to Protocols 2 and 3, except that the stirring element p_3 is absent. Although these protocols clearly both give rise to a trivial mathematical braid (because $m = 2$ in each case), they provide useful cases for comparison below.
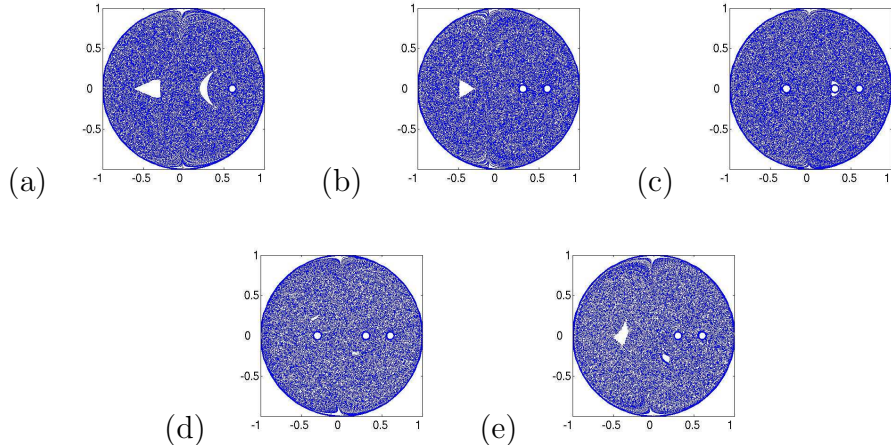
Fig. 2. Iterated mapping plots for the five Protocols studied. In all plots, the stirring elements have radius $a = 0.05$; $R = 0.30$ and $A = 0.60$. (a) Protocol 1; (b) Protocol 2*; (c) Protocol 2; (d) Protocol 3; (e) Protocol 3*.

4 Results

We use two diagnostics for assessing our stirring protocols. The first is the iterated mapping plot, or Poincaré section, in which we plot stroboscopically at times nT (for $n = 0, 1, \ldots, 1000$) the locations of a hundred passive tracer particles placed initially on a grid within the container. Regions of poor mixing are revealed as periodic islands; however, such plots are well known to have some significant shortcomings, for instance that they provide no information on the rate of separation of fluid particles in the chaotic sea. So in addition, motivated by the theoretical results above, we compute the stretch rate of a material line, dynamically inserting points to maintain adequate resolution as the line stretches [13]. With the length of the line at time t denoted by l_t, the mean stretch factor of the line per period of the flow is $\Lambda(t) \equiv (l_t/l_0)^{T/t}$, where the period T of the stirring protocols is normalized to $T = 1$.

We begin our discussion with Protocol 1, whose iterated mapping plot is shown in figure 2(a). (Note that in all simulations reported here, except those illustrated in figure 5, the stirring rod(s) and any baffles all have the same radius, here $a = 0.05$.) We see that although the bulk of the fluid is in a chaotic region, there are two periodic islands of poor mixing (one triangular, one a crescent). In figure 2(b), we show the effect of introducing a single stationary baffle into the flow (Protocol 2*), roughly at the location of the crescent-shaped island visible in figure 2(a). Notice that by the introduction of this baffle, we have significantly reduced the size of the central periodic island in figure 2(a), although the left-hand periodic island remains. (We have obtained qualitatively similar results by placing a single baffle instead in the left-hand island, at $R = -0.30$, in which case this island is essentially removed, but a visible central island remains.) Two stationary baffles (Protocol 2) considerably improve matters, as shown in figure 2(c) (this improvement was noted previously
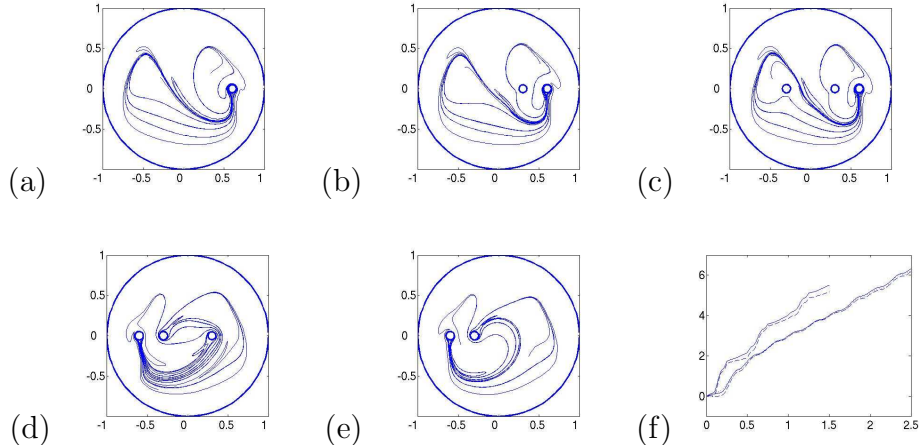
8

Fig. 3. Stretching of a material line in the five Protocols studied. Panels (a)–(e) correspond to figure 2 (i.e., are in the order Protocol 1, 2^*, 2, 3, 3^*); parameters are as used there. Initial line length is $l_0 = 0.40$. Length after stretching is: (a) $l_2 = 65.62$; (b) $l_2 = 61.91$; (c) $l_2 = 71.44$; (d) $l_{1.5} = 98.24$; (e) $l_{1.5} = 70.30$. The tremendous rate of stretch in (d) and (e) precludes well-resolved simulation of the line beyond roughly $t = 1.5$. (f) $\log(l_t/l_0)$ against time t, for each of (a)–(e). The lower dotted, dashed and solid curves are, respectively, for (a), (b) and (c), and are largely indistinguishable. The upper solid and dashed curves are for (d) and (e), respectively, and are significantly above those for (a), (b) and (c).

in [5]). Now both of the periodic islands have been essentially removed and visibly the global quality of the fluid mixing is better than in figures 2(a) and (b). Figure 2(d) corresponds to Protocol 3, which generates the pigtail braid; from a visual comparison of the iterated mapping plots in (c) and (d), there seems little to justify the additional complexity of Protocol 3 over Protocol 2. Finally, figure 2(e) shows the iterated mapping plot for Protocol 3^*, for which two significant islands are visible.

Figure 3 shows in panels (a)–(e) the effects of the fluid stirring upon a horizontal line whose endpoints are initially at $(\pm 0.20, 0)$. The initial length of the line is therefore $l_0 = 0.40$. In panels (a)–(c), the line is shown after two periods of stretching, although the extreme stretching for some parts of the line in panels (d) and (e) limits well-resolved simulations to approximately $t = 1.5$, so in these two cases the line is shown at this time (protocols and parameter values are as in figure 2). Figure 3(f) provides a quantitative comparison between the various protocols corresponding to panels (a)–(e), demonstrating the evolution of $\log(l_t/l_0) = t \log \Lambda$ with time. Protocols 1, 2 and 2^* stretch the line to a similar extent; for each we estimate $\Lambda \approx 10$. The two remaining protocols have $\Lambda \approx 29$ (Protocol 3, upper solid curve) and 26 (Protocol 3^*, upper dashed curve). Thus the rate of material line stretch is significantly better for Protocol 3 than for Protocols 1, 2 or 2^*, although only rather marginally better than for Protocol 3^*. The similar stretch rate for Protocols 1, 2 and 2^* is noteworthy, particularly since Protocols 1 and 2^* do not generate *robust* topological chaos, by which we mean that the stirring elements do not generate p-A mathematical braids (indeed, they *can* not, since they have, respectively,
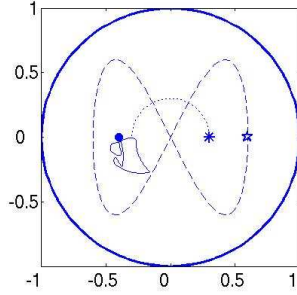
9

Fig. 4. Position of the stirring rod (five-pointed star) and fixed baffle (eight-pointed star) at times $t = n$ ($n = 0, 1, \ldots$) for Protocol 3*. The trajectories of the stirring rod and baffle are indicated by the dashed and dotted curves, respectively; that of the ghost rod is indicated by the solid curve.

$m = 1$ and 2 stirring elements.). It appears that the visible periodic islands in figure 2(a) and (b), which are barriers to material transport, act as effective (stationary) baffles, just as in figure 2(c). We confirmed this idea by tracking over a single period the trajectories of the periodic islands. For example, for Protocol 1, by considering there to be three stirring elements (the stirring rod together with the two islands), we find the braid word $\sigma_2^{-1}\sigma_1^2\sigma_2^{-1}$, which is pseudo-Anosov, with, from (1), $\lambda \approx 5.8$. Similarly, for Protocol 2* the three stirring elements are the stirring rod, the baffle and the large island. Again we find the braid word $\sigma_2^{-1}\sigma_1^2\sigma_2^{-1}$. This confirms that the periodic islands are indeed acting as proxy stirring elements, and leading to identifiable p-A braid words; they are "ghost rods" [12].

The reason for our introduction of Protocol 3* should now be clear. The aim of this protocol is to test whether the optimal pigtail braid might also be achieved with only one moving baffle, and with a periodic island (ghost rod) performing the role of the other baffle. Figure 2(e) indicates that when the left-hand baffle is removed from the optimal Protocol 3, a periodic island does indeed take its place. However, the periodic island, located near $(-0.40, 0.00)$ in figure 2(e), does not move in the same way as the physical rod does in the optimal protocol; indeed, it does not move out of the left-hand lobe of the figure-of-eight (see figure 4). The corresponding braid word generated by the two stirring elements together with the ghost rod then turns out to be $\sigma_2\sigma_1\sigma_2\sigma_2^{-1}\sigma_1\sigma_2^{-1}$, which is equivalent to the trivial σ_1^2. If we consider instead both this ghost rod and one generated by the periodic island located at approximately $(0.15, -0.27)$ in figure 2(e) then we find instead a nontrivial braid word, $\sigma_2\sigma_3^{-1}\sigma_2\sigma_1^2\sigma_2^{-1}\sigma_3^{-1}\sigma_2^{-1}$, which has $\lambda \approx 5.83$ (this value was computed using Bestvina and Handel's [3] train-track algorithm, as implemented in the C++ code of Toby Hall, University of Liverpool; it is known that the matrix representation described above gives only a lower bound on λ when more than three stirring rods – or baffles or ghost rods – are involved, so the more sophisticated calculation is required). The true stretch-per-period is considerably greater than this value, and so we surmise the existence of further, smaller ghost rods, which are responsible for the observed stretch rate (cf. [12]). We

a_j	A	Λ_1	Λ_3	Λ_{3*}
0.05	0.60	10	29	26
0.05	0.50	6.5	19	18
0.03	0.50	7	29	28.5
0.03	0.60	10	39.5	38.5
0.07	0.60	8	24.5	22

Table 1

Stretch factors: Λ_1 (for Protocols 1, 2 and 2*, which, to the precision given, all have the same value of Λ), Λ_3 and Λ_{3*} (for Protocols 3 and 3*), for five different parameter choices. In all cases, $R = 0.30$, and all stirring rods/baffles have radius as indicated in the column headed a_j.
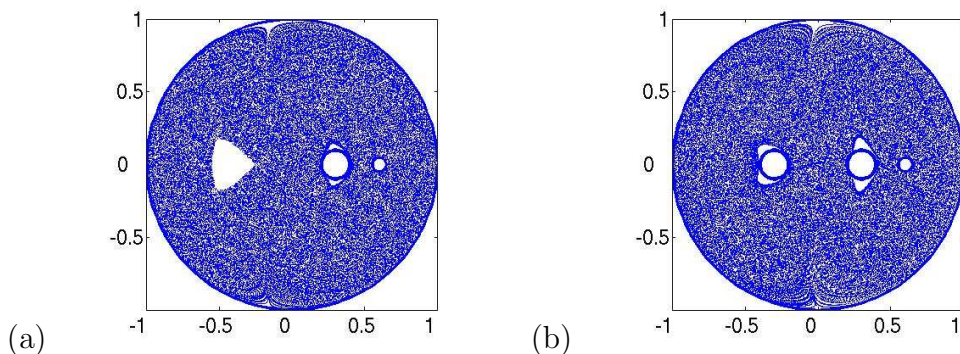

(a)   (b)

Fig. 5. Iterated mapping plots: (a) for Protocol 2*, with $a_1 = 0.05$, $a_2 = 0.10$, $A = 0.60$ and $R = 0.30$; (b) for Protocol 2, with $a_1 = 0.05$, $a_2 = a_3 = 0.10$, $A = 0.60$ and $R = 0.30$. These plots thus (respectively) correspond to figure 2(b) and (c), but with an increased radius for the baffle(s).

have not attempted to find such ghost rods, largely because of the computational cost of doing so. To illustrate this potentially high cost, we mention that Gouillart et al. [12] found orbits up to period nine to be necessary in determining a reasonably accurate approximation to the observed stretch rate (this result was obtained for a single stirring rod – and multiple ghost rods – for which the velocity field is known analytically).

We find a similar qualitative picture for other parameter values, although we have been unable to deduce any general trends as, say, A, R and the a_j are varied. A sample of results for the stretch factor Λ is given in table 1 (the first line of data there corresponds to the simulations described in detail above). For example, we find that repeating the calculations described above with $A = 0.50$ instead of 0.60 generates a similar qualitative picture, but with smaller ghost rods and smaller Λ. Variations to the radii of the stirring rods and baffles likewise lead to similar qualitative results. For example, figure 5 shows the effects upon Protocols 2* and 2 of increasing the baffle radius (keeping all other parameters as in figure 2(b) and (c)). When there is only a single baffle, as in figure 5(a) and figure 2(b), it is rather intriguing that the larger baffle

leads to a larger ghost rod. Similarly, when there are two baffles, an increase in the baffle radius increases the size of the (small) regular region around each baffle.

5   Conclusions and discussion

We have demonstrated a practical means of achieving the optimal pigtail braid in a batch mixing device, and shown that it outperforms similar constructions that do not generate the pigtail braid, at least in the numerical simulations of Stokes flow that we have carried out.

An earlier and simpler design of a batch mixer (our Procotol 2) also generates a topologically nontrivial braid, but it does not achieve the pigtail braid. Protocol 2 is, however, interesting because either stationary baffle – or, indeed, both – may be removed and in a wide range of simulations for different parameter values (not reported in detail here) flow structures form "proxy" baffles (the "ghost rods" of [12]), so that the nontrivial braid is maintained, and the material line stretch rate is largely indifferent to the presence or otherwise of the physical baffles. Of course, the existence or otherwise of ghost rods — and the details of their associated braiding motions — must be determined on a case-by-case basis, in contrast to stirring protocols with $m \geq 3$ where the relative motions of the stirring rods and baffles can be designed to enact a nontrivial braid.

A similar attempt to remove one of the baffles from our optimal design fails because, although a periodic island forms to replace the omitted baffle, it does not move appropriately, and the pigtail braid is lost.

We note that, in all cases, the actual line stretch rate is far in excess of that predicted by the braid word that forms the basis of the mixer design. Such a result is consistent with corresponding results of Gouillart et al. [12], who found that high-period (and small) islands may need to be considered to predict accurately the observed stretch rate.

Acknowledgements

References

[1] Aref, H., 1984. Stirring by chaotic advection. J. Fluid Mech. 143, 1–21.

[2] Aref, H., 2002. The development of chaotic advection. Phys. Fluids 14, 1315–1325.

[3] Bestvina, M., Handel, M., 1995. Train-tracks for surface homeomorphisms. Topology 34, 109–140.

[4] Boyland, P.L., Aref, H., Stremler, M.A., 2000. Topological fluid mechanics of stirring. J. Fluid Mech. 40, 277–304.

[5] Clifford, M.J., Cox, S.M., 2006. Smart baffle placement for chaotic mixing. Nonlinear Dynamics 43, 117–126.

[6] Clifford, M.J., Cox, S.M., Finn, M.D., 2004. Reynolds number effects in a simple planetary mixer. Chem. Eng. Sci. 59, 3371–3379.

[7] D'Alessandro, D., Dahleh, M. and Mezić, I., 1999. Control of mixing in fluid flow: a maximum entropy approach. IEEE Trans. Automatic Control 44, 1852–1863.

[8] Finn, M.D., Thiffeault, J.–L., Gouillart, E., 2005. Topological chaos in spatially periodic mixers. Physica D, in press, and arXiv:nlin.CD/0507023.

[9] Finn, M.D., Cox, S.M., Byrne, H.M., 2004. Mixing measures for a two–dimensional chaotic Stokes flow. J. Eng. Math. 48, 129–155.

[10] Finn, M.D., Cox, S.M., 2001. Stokes flow in a mixer with changing geometry. J. Eng. Math. 41, 75–99.

[11] Finn, M.D., Cox, S.M., Byrne, H.M., 2003. Topological chaos in inviscid and viscous mixers. J. Fluid Mech. 493, 345–361.

[12] Gouillart, E., Thiffeault, J.–L., Finn, M.D., 2006. Topological mixing with ghost rods. Phys. Rev. E 73, 036311.

[13] Krasnopolskaya, T.S., Meleshko, V.V., Peters, G.W.M., Meijer, H.E.H., 1999. Mixing in Stokes flow in an annular wedge cavity. Euro. J. Mech. B/Fluids 18, 793–822.

[14] Lamb, H., 1932. Hydrodynamics, 6th edn., Cambridge University Press.

[15] Mackay, R.S., 2001. Complicated dynamics from simple topological hypotheses. Phil. Trans. R. Soc. Lond. 359, 1479–1496.

[16] Thiffeault, J.–L. and Finn, M.D., 2006. Topology, braids, and mixing in fluids. arXiv:nlin.CD/0603003.